Dynamic *in situ* optical and magneto-optical monitoring of the growth of Co/Au multilayers

R. Atkinson, G. Didrichsen, W. R. Hendren, I. W. Salter, and R. J. Pollard

The Queen's University of Belfast, Department of Pure and Applied Physics, Belfast BT7 1NN, United Kingdom

(Received 27 January 2000; revised manuscript received 1 May 2000)

In situ ellipsometry and Kerr polarimetry have been used to follow, continuously, the evolution of the optical and magneto-optical properties of multiple layers of Co (5 Å) and Au (37.5 Å) during their deposition. A particular feature of the results shows marked oscillations of the magneto-optic polar Kerr effect, with a period of about 16 Å, during the deposition of each Au layer. The appearance of oscillations occurs in both Kerr ellipticity and rotation in a way that depends upon underlying buffer layer thickness and the number of bilayer periods in the multilayer stack. Magneto-optical oscillations have been reported previously in Co/Au and Fe/Au systems and have been interpreted as being a consequence of magneto-optic transitions associated with quantum-well states in the noble-metal layer. The comprehensive optical and magneto-optical measurements reported here allow intrinsic material properties to be determined for developing ultrathin layers. These facilitate a better understanding of the observed magneto-optical signals that result from such structures and also provide a means of predicting such signals for any optical system.

I. INTRODUCTION

Considerable attention has been given recently to the optical, magneto-optical, and magnetic properties of multilayered systems, where individual film thicknesses are typically a few atoms thick.[1–5] It is intuitively obvious that the electronic structures of very thin films may differ significantly from those of the bulk and that this may be reflected in the physical properties of the material, including the optical and magneto-optical properties.[6] Indeed, several theoretical and experimental studies have been made of the properties of multilayer systems that show strong evidence for properties that cannot be explained on the basis of bulk data.[7,8] One of the more remarkable aspects of these studies is concerned with oscillations in the magneto-optic effects observed when transition-metal layers are combined with noble metals.[9,10] Such observations are often made *ex situ*, using wedged ultrathin layers, and for this reason are subject to uncertainties that may arise because of contamination and interdiffusion. Moreover, any dynamic information that could give clues to the film growth process and evolution of properties is totally lost.

The authors have recently carried out a comprehensive study of the growth of several multilayer systems using *in situ* optical, magneto-optical, and magnetic diagnostics to follow the evolving properties of the structures in real time. This paper reports on observations and analysis of the CoAu system. This system is particularly interesting since it has been reported that magneto-optical transitions, not seen in the bulk, occur in CoAu and FeAu structures and that such transitions are dependent on the Au interlayer thickness. Having said that, it must be emphasized that it is possible to confuse intrinsic magneto-optical transitions with variations (oscillations) in observed Kerr effects that have their origin in the optical environment in which the magnetic layer finds itself. This situation is exacerbated by the fact that typical magneto-optic line shapes, whether paramagnetic or diamagnetic in origin, often resemble those that may be produced by optical means and which, of course, are not intrinsic to the

material itself.[11,12] In general and particularly in situations where film properties may be thickness dependent, it is expedient, when trying to understand magneto-optical observations, to have a firm grasp of the evolving optical properties of the system as a whole, as well as the magneto-optical properties, since the former may have a significant influence on the latter. Additionally, magneto-optical data should be comprehensive and include, for example, measurements of both Kerr rotation and ellipticity, since it is only from such complete data that complex information about intrinsic material properties can be inferred. In these dynamic, *in situ* observations of the CoAu system one sees, in real time and with great clarity, oscillations in the normal incidence polar Kerr effect and how these change in character as multiple bilayers are added to a growing structure. Complementing the magneto-optic data detailed information is presented on the evolving optical properties of the system. The two are, of course, related.

II. EXPERIMENT

Figure 1 shows a schematic diagram of the deposition chamber and associated monitoring equipment. Two PC-controlled, planar rf magnetrons were used to sputter deposit Co and Au multiple layers onto glass substrates at room temperature in an Ar pressure of $\sim 2.2 \times 10^{-3}$ mbar.

In situ optical and magneto-optical monitoring, at a wavelength $\lambda = 6328$ Å, was achieved using a fast, rotating analyzer ellipsometer and a normal incidence Kerr polarimeter. The ellipsometer, operating at an angle of incidence of 69.5°, was used to determine the optical functions $\text{Re}(r_p/r_s)$ and $\text{Re}(r_s/r_p)$, where r_p and r_s are the complex Fresnel amplitude reflection coefficients for *P*- and *S*-polarized light, respectively. Complete data sets were obtained each second during the deposition period. Individual measurements were completed within 100 ms.

The Kerr polarimeter, based on the use of a photoelastic
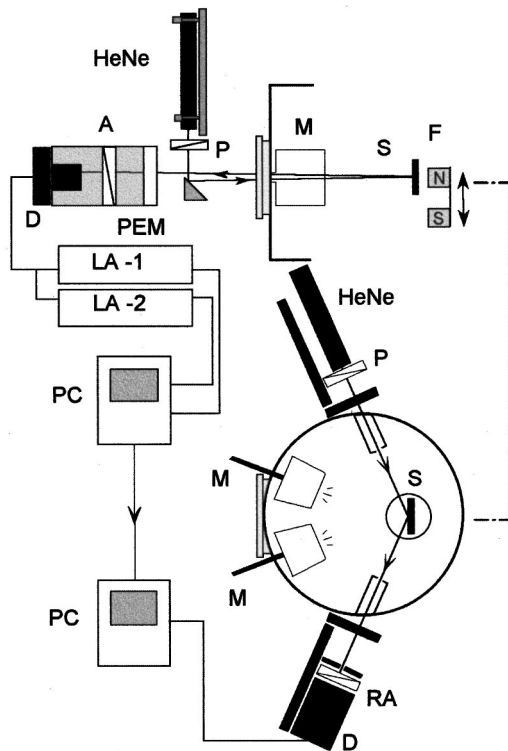
FIG. 1. Schematic diagram of the deposition system. HeNe, helium neon laser; *A*, analyzer; *P*, polarizer; RA rotating analyzer; PEM, photoelastic modulator; *M*, magnetron; PC, computer; *S*, substrate; *D*, detector; La-1, lock-in amplifier (50 kHz); LA-2, lock-in amplifier (100 kHz); *F*, field switch.

modulator (PEM) operating at 50 kHz, allowed the simultaneous measurement of both Kerr rotation and ellipticity with precisions better than ±5 and ±1 arc sec, respectively, limited by mechanical vibrations rather than shot noise or laser instabilities. The details of this technique have been well described previously.[13] Radiation incident on the sample, at less than 0.5°, was ensured to be linearly polarized by the use of an aluminum reflector and the choice of the orientation of the primary polarizer with respect to the plane of incidence of the mirror. All films were deposited in an applied perpendicular field of 0.28 T, produced by permanent magnets that could be reversed automatically if required. All optical windows into the vacuum system were manufactured, in house, from carefully selected low-stress optical coefficient glass.

Two synchronized computers coordinated the deposition and data-collection sequence. These controlled the magnetron shutters, magnetic field switching, and the status of a quartz crystal monitor as well as the operation of the ellipsometer and all data collection during the deposition.

III. RESULTS

In this section both the optical ellipsometric results and the magneto-optical data are presented as a function of time or film thickness during the deposition of ten (CoAu) bilayers on a 125-Å Au buffer layer on glass. The buffer layer thickness was carefully selected to satisfy two criteria: first, that the layer be physically continuous, and second, that it be as thin as possible to provide the minimum reflectivity and, hence, maximum magneto-optical effects. It is emphasized
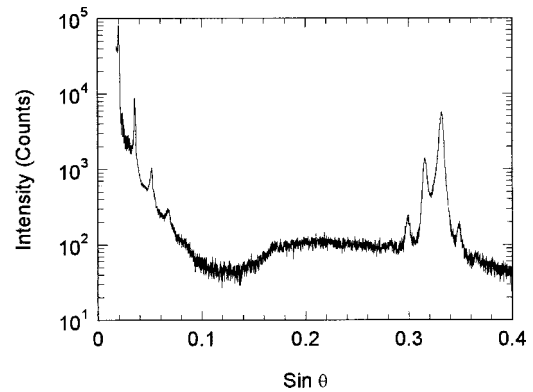
FIG. 2. Typical XRD peaks for Co/Au multilayers on a 125-Å Au buffer layer on glass.

that a single set of observations is presented, though this is typical and has been repeated several times with good reproducibility.

A. Optical

Figure 2 illustrates the x-ray diffraction pattern that is typical of the CoAu multilayers deposited in this series of experiments. The appearance of several low-angle peaks associated with the bilayer periodicity confirms a well-defined layered structure as do the high-angle peaks centred around the position of the Au(111) peak. Corresponding to such systems, Fig. 3 shows the ellipsometric data $Re(r_p/r_s)$ and $Re(r_s/r_p)$ as a function of increasing total film thickness obtained during the deposition of a glass/125 Au/10 (5Co/37.5 Au) system. From such data it is possible, in the first instance, to determine the refractive index of the Au buffer layer and the effective [single equivalent layer (SEL) (Ref. 14)] refractive index of the CoAu multilayer, treated as a single layer. This is done using the data points after 125 Å and at the end of the deposition. The results allow one to calculate the complete growth curves of Fig. 3, assuming a simple two-layer system, the CoAu multilayer being considered isotropic and homogeneous. Despite the simplicity of the model, the calculation is seen to fit the observations very well. The only exception occurs at the early stages of the deposition of the Au buffer layer where there are marked differences between both observations and their predictions.
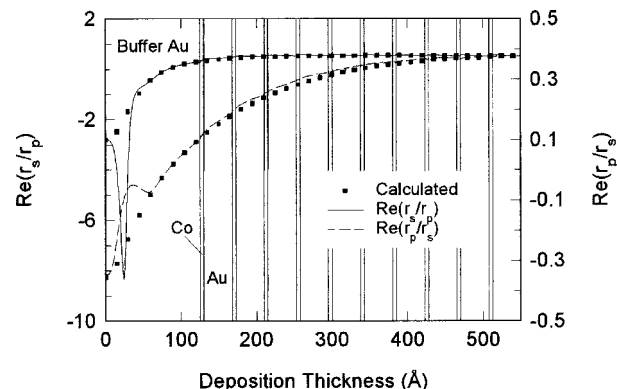
FIG. 3. Ellipsometric measurements of $Re(r_p/r_s)$ and $Re(r_s/r_p)$ at $\lambda = 6328$ Å, together with calculated values using a simple two-layer system.
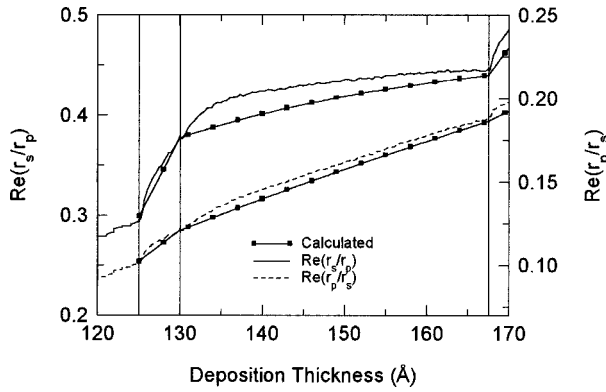
FIG. 4. Ellipsometric measurements of $Re(r_p/r_s)$ and $Re(r_s/r_p)$, at $\lambda = 6328$ Å, for the first bilayer. Curves with markers indicate calculations assuming a fixed refractive index for the gold.

These differences are not important from the point of view of the subject matter here. However, they can be explained using Maxwell-Garnet theory applied to a situation where the Au film is nucleating, by a process of cluster formation, on the glass substrate and that this nucleation process may be modified by the application of *in situ* ion-beam cleaning of the substrate prior to the deposition process.[15]

From these observations the refractive index of the Au buffer layer is determined to be $\hat{n}_{buf}(=0.176 + i3.909)$ and that of the effective CoAu multilayer $\hat{n}_{CoAu}(=0.70 + i3.86)$. Assuming that the index for each gold layer is equal to $\hat{n}_{buf}$ and using the SEL theory, this indicates a refractive index for the Co layer of $\hat{n}_{Co}(\approx 3.9 + i4.7)$. In the case of $\hat{n}_{buf}$ this is close to that of thick Au films and any discrepancies may be accounted for by the fact that the layer is only 125 Å thick and that these measurements were made *in situ* and were not subject to external contamination. In the case of Co, the inferred index is a little different from the thick film value. This is to be expected since the layer is only a little over one monolayer thick and the thickness of the accompanying Au layer is rather larger than one would consider acceptable for full applicability of the SEL model.[14] Nevertheless, the effective index is a reasonable indication of what one might expect for such an ultrathin layer of Co.

B. Detailed optical observations

In order to illustrate the sensitivity of the ellipsometric data an enlarged section of Fig. 3, corresponding to the first bilayer, is shown in Fig. 4. It is clear from Figs. 3 and 4 that there are distinct modulations in the optical data that correspond to the depositions of the separate Co and Au layers. From these data it is possible to determine the effective refractive indicates of each completed layer. In this case $\hat{n}_{Co}(=3.47 + i5.10)$ and $\hat{n}_{Au}(=0.23 + i3.92)$. It should be noted that these are in good agreement with those deduced from the full set of curves of Fig. 3 combined with the SEL model. Using these parameters, the detailed curves for the full growth period are calculated and shown in Fig. 4.

The level of agreement between the measured and calculated curves of Fig. 4 is good, and if the whole ten bilayer periods were to be presented in a single graph, the calculated and measured modulated curves would look impressive. However, at the magnification shown in Fig. 4, there are
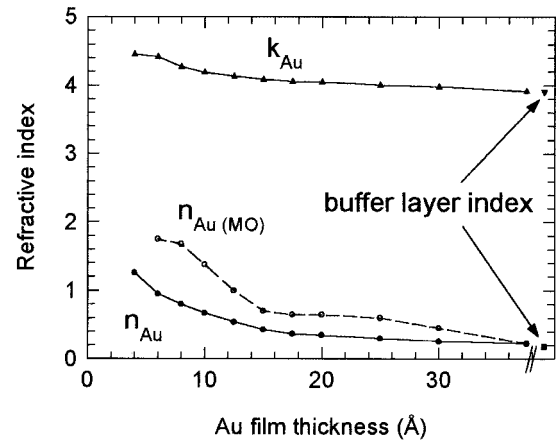
FIG. 5. Variation of the complex refractive index of Au with thickness. Solid curves from ellipsometry, dotted curve from fitting of Kerr ellipticity data. The isolated points correspond to the values for the buffer layer.

discrepancies between the curves. These differences are crucially important and, though small, indicate that the refractive index of the Au layer is changing with film thickness and most of this change occurs in the range from 0 to about 40 Å. This also accounts for the small systematic difference between the $\hat{n}_{Au}$ and $\hat{n}_{buf}$. The variation is clearly seen in the solid curves of Fig. 5 where, using the ellipsometric data of Fig. 4, the refractive index of the Au layer has been calculated as a function of film thickness for the first bilayer. The index of the buffer layer is also indicated in Fig. 5, for comparison, where it can be seen that extrapolation of the Au thickness up to 125 Å would provide very good agreement between the two sets of data.

C. Temporal optical observations

With other multilayered materials it has proved expedient to examine any temporal variations in the *in situ* data to eliminate the possibility of several undesirable effects such as instrumental drift, the deposition of extraneous material during periods when both shutters are closed, or the possibility of interlayer diffusion or film restructuring, on time scales comparable to the deposition period. The latter, of course, provides additional valuable data on the dynamics of film formation.

In this work, temporal studies were carried out separately for both optical and magneto-optical data. Figure 6 shows a curve, typical of the CoAu system, where a time delay of 80 s has been introduced after the deposition of the, relatively fragile, Co layer. It is clear from the optical data of Fig. 6 that the constant values of optical functions during the delay period of 80 s shows that the system is remarkably stable, both instrumentally and as a material system. It may be concluded therefore that, as far as the optical data is concerned, there are no significant signs of contamination or interdiffusion of materials. Indeed, if the time delay sections are removed, the remaining curves appear identical to those shown in Fig. 4. It is also pointed out that time delays inserted after the deposition of the Au layers show an identical behavior.

On the basis of the optical data alone, one may conclude that the system is relatively stable, well defined, in terms of the individual layers, and that there is no significant interdif-
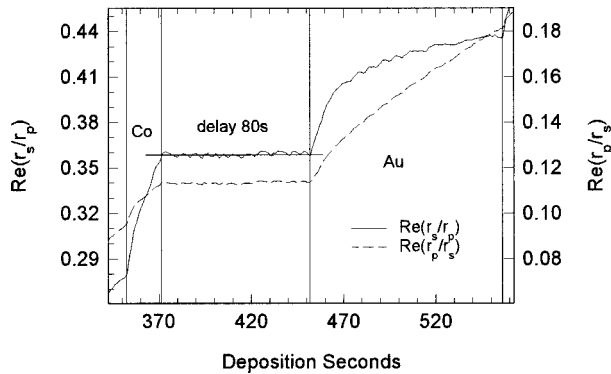
FIG. 6. Temporal variation of the ellipsometric data during an 80-s delay between the deposition of a Co-Au bilayer. (The horizontal line is to guide the eye.)

fusion of materials. Moreover, and importantly, the optical properties of the individual Au layers are markedly thickness dependent over the thickness range 0–40 Å and approach those of the buffer layer that are in good agreement with the usual optical constants of thin film Au. The optical constants of Co, on the other hand, differ substantially from bulk values. However, it should be remembered that the layer is a little over a monolayer thick and therefore cannot be expected to have bulklike properties. Indeed, the optical properties could also depend upon the underlying material.

D. Magneto-optical observations

Before presenting the magneto-optical data, it is necessary to establish the orientation of the magnetization that is associated with the growing multilayer. In the CoAu system this moment is entirely associated with the Co atoms. It has been shown previously[16] that, provided the Co layer is not too thick, the moment is perpendicular to the film surface when deposited on a Au surface. *Ex situ* hysteresis loops on our completed ten-bilayer systems also confirmed this. Figure 7 shows a typical perpendicular loop for the completed system. The sensitivity for the *ex situ* hysteresis loop plotter is much lower than that for the *in situ* Kerr polarimeter. In addition, it should be remembered that all layers were deposited in an applied magnetic field of 0.28 T, which was present during the continuous measurement of the evolving polar magneto-
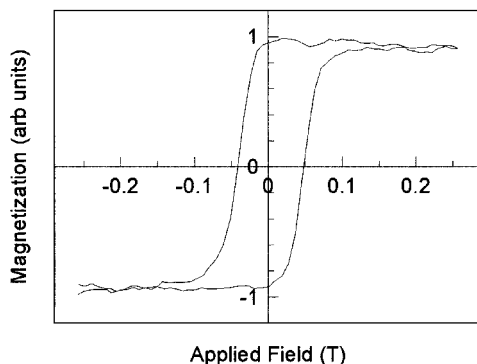
FIG. 7. *Ex situ*, perpendicular, hysteresis loop for a glass/125 Au/10 (5 Co/37.5 Au) multilayer that corresponds to the *in situ* data presented in this work.
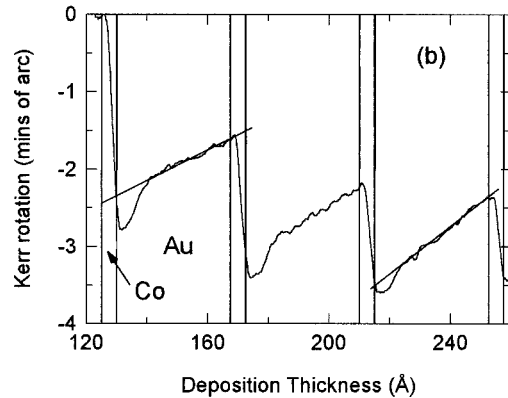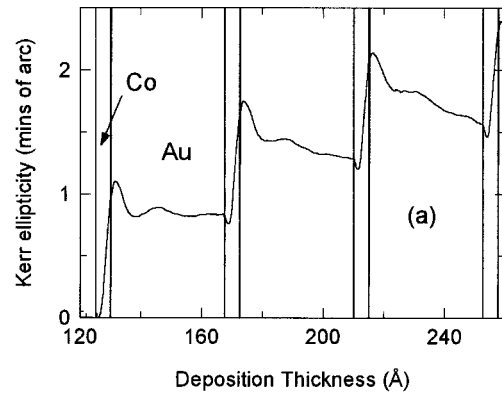
FIG. 8. Measured variation of the polar Kerr ellipticity (a) and rotation (b), during the deposition of the first three bilayers of a glass/125 Au/10 (5 Co/37.5 Au) multilayer. (The straight lines are a guide for the eye.)

optic effects. The magnetization of the Co is therefore assumed to be in a state of saturation, perpendicular to the film plane, for all measurements.

Figures 8(a) and 8(b) shows the magneto-optical data for the first three bilayers in the system. Beyond this, the pattern is repeated with gradually increasing rotation and ellipticity that is entirely consistent with the principal of magneto-optic superposition[17] and increasing overall film thickness. Readers should note that the preferred sign convention for magneto-optical effects and parameters has been adopted and is defined fully elsewhere.[18]

There are several features of the curves of Fig. 8 that are important and these are enumerated below for convenience.

(1) The two curves represent the continuous, real-time, monitoring of the polar Kerr effect during the deposition of the layers. Any instrumental drift, and this is usually small or negligible, has been removed.

(2) The noise on the rotation signal is larger than that on the ellipticity since the latter is a phase-dependent measurement and, naturally, not affected by system vibrations to the same extent as rotation.

(3) The deposition of the Co layer is characterized by a sudden large increase in both magneto-optic signals. However, it should be noted that the onset of this signal does not occur until a critical thickness of about 1.6 Å has been deposited.

(4) On the deposition of the Au layer, there is a small initial increase in both signals, though this feature gradually disappears as successive bilayers are added.
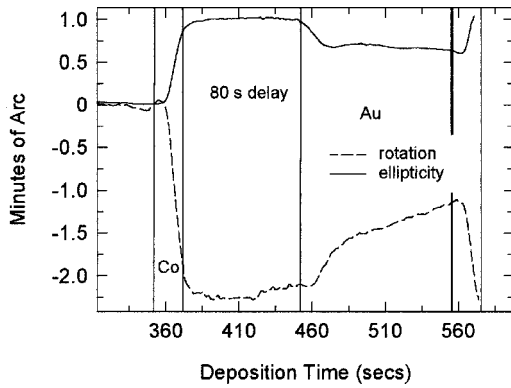
FIG. 9. Temporal variation of the complex polar Kerr effect during an 80-s delay between the deposition of the Co and Au in the first bilayer.

FIG. 10. Theoretical fit (open markers) to the observed Kerr effect for the first three bilayers, assuming fixed optical constants for the gold layer.

(5) The decrease in Kerr rotation produced by the Au is, more or less, linear for the major part of the deposition.

(6) In the case of Kerr ellipticity, the deposition of the Au induces marked oscillations that are repeated in each successive bilayer. The thicknesses at which the main turning points occur are approximately 8, 16, and 25 Å, and this is most clearly seen in the first bilayer. Subsequent bilayers also show these features, but the increasing overall system thickness operates optically (increasing reflectance) to reduce the clarity of the turning point at 25 Å.

(7) The extrapolation of the linear section of each Kerr rotation curve intersects with the Kerr rotation value associated with the end point value after the deposition of the Co layer. A similar point can be made for ellipticity, though this is less clear because of the oscillatory nature of the curves.

E. Temporal magneto-optical observations

Figure 9 shows the variation of the measured Kerr effects for an 80-s delay period after the deposition of the Co layer. A similar delay after the deposition of the Au layer shows no changes. The importance of these curves lies in the changes that take place while the freshly deposited Co surface is exposed to the ambient atmosphere of the deposition system. In the case of the rotation, this corresponds to a small increase. Thereafter, the changes are monotonic towards the linear section. Likewise, in the case of ellipticity there is an initial small increase followed by a monotonic decrease that begins on the deposition of Au. This is followed by clear oscillations.

IV. DISCUSSION

The above observations, both optical and magneto-optical, contain a wealth of detailed information that must be internally self-consistent and explicable in terms of the growth processes and possible changes in electronic configurations of the materials being used. In order to do this it is instructive, first, to explore the simplest case, where it is assumed that the Co and Au layers are perfect plane layers of well-defined boundaries and fixed, thickness-independent, optical and magneto-optical constants. The constants referred to are the complex refractive indices $\hat{n}(=n+ik)$ and the complex magneto-optic Voigt parameter $\hat{Q}(=Q_1+iQ_2)$,
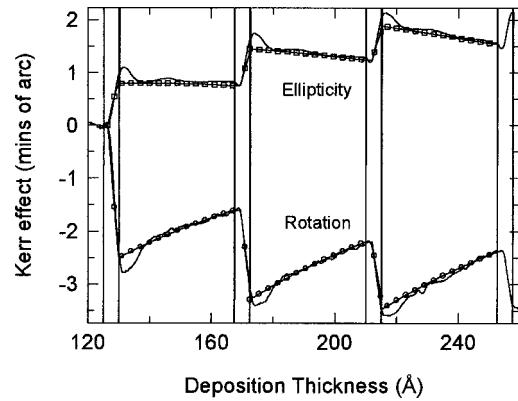
which appears as an off-diagonal component in the skew-symmetric tensor of a gyroelectric medium.[11] The former were determined earlier, and the latter may be obtained from the Kerr rotation and ellipticity angles. In order to do this it is necessary to determine what these values are. Given the temporal variations shown in Fig. 9 and the extrapolations, particularly in the case of the linear sections of the rotation curves in Fig. 8, it is felt that the best estimates correspond to the values measured at the end of the Co deposition and this leads to a value for Co $\hat{Q}_{Co}(=-0.0144+i0.0035)$. Any other choice is slightly problematic since it cannot be determined whether any other value is a consequence of the deposition of Au or the exposure of the Co to the residual ambient atmosphere in the chamber. In any case, the differences between the various options are quite small and would not lead to any changes in the general conclusions of this work. Nevertheless, this decision has been considered carefully and is supported by a comparison of the measured data with calculations based on various models. The results for the simplest of these models, outlined above, are shown in Fig. 10.

It is clear from Fig. 10 that the general agreement between the simple model and the measured data is very good. The match with the linear sections of rotation of all three bilayers is excellent and, disregarding the absence of the oscillations in ellipticity, the agreement here is also good. It should be borne in mind, when comparing these data, that all optical and magneto-optical constants have been determined from ellipsometry and Kerr polarimetry on the first bilayer only. In addition, it should be noted that the start of magneto-optical activity in the Co layer has been deliberately shifted from zero to 1.6 Å to coincide with the observations. The reason for this may be understood from the growth mechanism of Co on Au that proceeds by[16] cluster formation up to the first monolayer. Since ferromagnetism is a collective phenomenon, the onset of magneto-optic signals is delayed until sufficient material has been deposited to trigger the ferromagnetic properties. Prior to this, of course, Co atoms are being deposited continuously, as can be seen from Fig. 4, where the optical signals commence immediately the Co source shutter is opened. Further evidence of this is discussed later.

Despite the general agreement obtained, the details of the Kerr data are yet to be explained, particularly in relation to the oscillations seen in the ellipticity signal. In order to begin
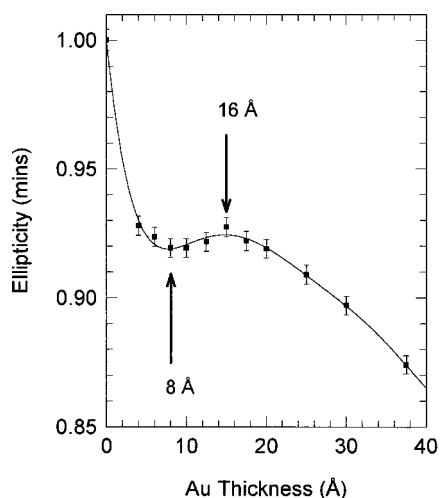
FIG. 11. Calculated points for the ellipticity of the first bilayer using the variable refractive index of Au derived from ellipsometric data. (The continuous curve is fitted to the points.)

to explain this, we must return to the optical results, where there is clear evidence that the effective refractive index of the Au layer is thickness dependent. This is now be taken into account in the calculation of the evolving Kerr signal and the results are given in Fig. 11 where the calculated Kerr ellipticity is shown for the first bilayer, taking into account the variable Au index determined from the ellipsometric results. The error bars shown are estimated from the random uncertainties in the calculated values of the index.

With regard to this figure a number of points are important. First, there is a rapid initial decrease in ellipticity that qualitatively agrees with what is seen in the measured data. Second, two clear turning points follow, at approximately 8 and 16 Å, which coincide with the dynamic measurements. The reader should compare the curve of Fig. 11 with those associated with the various bilayers given in Fig. 8(a). It should also be noted that in the case of the Kerr rotation the results of these modified calculations remain virtually identical to those carried out previously. That is, no oscillations are predicted. For this reason they are not shown. This latter point is important since it is an indication that the variable index of the Au layer affects the Kerr ellipticity and not the rotation, which is what is observed experimentally, at least for the first bilayer.

The ability of the optical and magneto-optical calculations to predict the existence and positions of these oscillations was unexpected. There is, however, one drawback to the values calculated and shown in Fig. 11. While the general form of the oscillatory curve is encouraging and the location of the peaks is good, the depth of modulation does not correspond with that observed. This could be due to small systematic errors in the ellipsometric measurements combined with small uncertainties in the various film thicknesses in the system. It should be remembered that the variation of index for the Au layer is taken from a highly magnified section (Fig. 4) of the ellipsometric data (Fig. 3) and these data have been collected dynamically in real time through two vacuum windows that, despite precautions, may have problems of ill-defined strain birefringence that could alter the ellipsometric polarization parameters.

Because of this result, an attempt was made to estimate
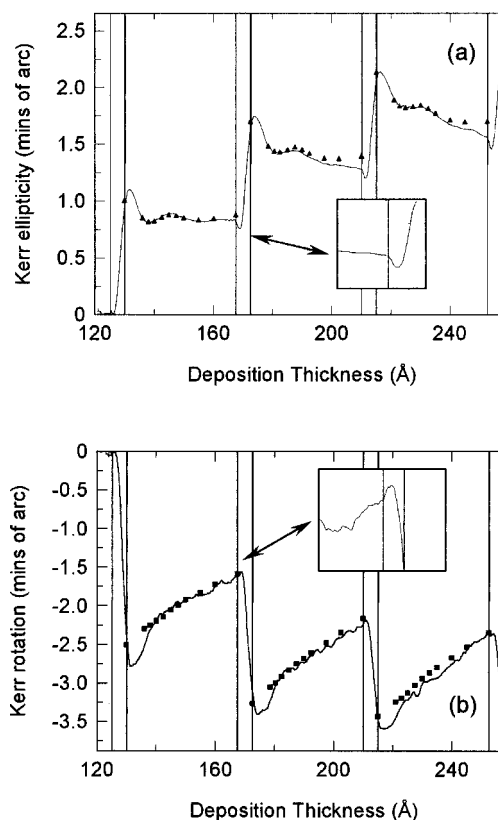
FIG. 12. Theoretical calculation (solid markers) of the complex Kerr ellipticity (a) and rotation (b) for the first three bilayers using the variable refractive index of Au derived from the ellipticity of the first bilayer.

what variation in Au index would be required to account for the observed oscillations. To do this a simple data fitting procedure was carried out, restricted to a single variable, namely, the real part n_{Au} of the refractive index of the Au layer as a function of thickness. The decision to do this is based upon two observations. First, the fitting of ellipticity and rotation in the above model is seen to be relatively insensitive to the imaginary part of the refractive index k_{Au}. For this reason the fixed values given in Fig. 5 were assumed. Second, the measured variation of k_{Au} with film thickness is very small (10%) compared to that for the real part, which is greater than 800%. Finally, it is emphasised that n_{Au} is adjusted to fit the oscillations in ellipticity only. Following this, the associated rotations are calculated, as a test, to be compared with the observations. The results of this procedure are illustrated in Figs. 12(a) and 12(b). The corresponding values of n_{Au} are also shown, for comparison in Fig. 5.

Figure 12 shows the original Kerr signals together with the calculated values that result from the fitting of the Kerr ellipticity on the first bilayer. The agreement of the ellipticity on the first bilayer is, of course, ensured. However, it is clear that the new values of n_{Au}, when applied to subsequent bilayers, provide excellent agreement in positioning the turning points and their absolute values. Importantly, it should be noted that these calculations also provide agreement with the Kerr rotations, at least over the linear section, and indicate no oscillations. The variation of the Au index that produces these results reasonably follows that determined by ellipsom-

etry, though it must be stated that there is a little structure in these variations that is absent in the previous data. Nevertheless, given the overall arguments presented and the similarities of the curves, it is considered that the values are not unreasonable and may reflect, more truly, the actual variations in the growing Au layer. It is worth noting that, if these constants are used to calculate the measurable ellipsometric functions and if these are mapped back onto Fig. 4, the results are very close to the observed curves.

There remain some additional points, in relation to the magneto-optical observations, that should be discussed briefly. First, none of the calculations account for the initial rapid rise and decay of Kerr effect that is seen in the experimental observations as the Au is deposited. However, it should be remembered that this effect is also observed (Fig. 9) when the film is left exposed to the ambient atmosphere of the deposition chamber. It is therefore concluded that reordering of the Co atoms is a more likely explanation and that this may be induced through bombardment by residual gas atoms, which takes a matter of a few tens of seconds, or, more quickly, by bombardment from depositing Au atoms. Whatever the cause, the effect does not seem to be particularly related to the Au film itself.

Second, attention is drawn to the two insets in Fig. 12. These show magnified sections of the deposition of the Co atoms in the second bilayer, though they apply to all subsequent bilayers. These details may be understood in terms of the delay of the onset of the magnetic properties of the Co. In each case (ellipticity and rotation) there is no increase in the magneto-optical effect until approximately 1.6 Å has been deposited. What is also clear is that, until this point is reached, the addition of nonmagnetized Co acts like any other optically absorbing medium in reducing the magneto-optic signal from the underlying material. In consequence, a small dip in the ellipticity signal is seen in Fig. 12(a) and an extension of the decreasing linear section for rotation in Fig. 12(b), prior to the onset of additional magneto-optic activity from the growing Co layer as its ferromagnetic properties switch on. This observation is related to the growth of Co on Au that proceeds by cluster formation of increasing size such that, at the equivalent of 1.6 Å, the clusters are large enough for the collective ferromagnetic properties to become effective. Below this the clusters are too small and are either paramagnetic or superparamagnetic.

The interpretation of oscillations in Kerr ellipticity as resulting from variations in the refractive index of the Au layer is, at the very least, convenient from the point of view of predicting the magneto-optical behavior of these structures and, so far, it has been demonstrated to be effective. Nevertheless, the idea appears to conflict with previous conclusions[9,19–22] that these are intrinsically magneto-optic in origin. In addition, previously reported measurements have shown oscillations in Kerr rotation and not ellipticity. Both of these issues require consideration and explanation.

One of the significant achievements of previous work on the FeAu system[20] has been to relate oscillatory periods to photon energy through the concept of spin-polarized quantum size effects in the Au layer. However, if such quantum levels in the Au layer have an influence on the optical properties of the Au itself, then the inevitable result would be an oscillatory effect of the same period. Indirectly, this would
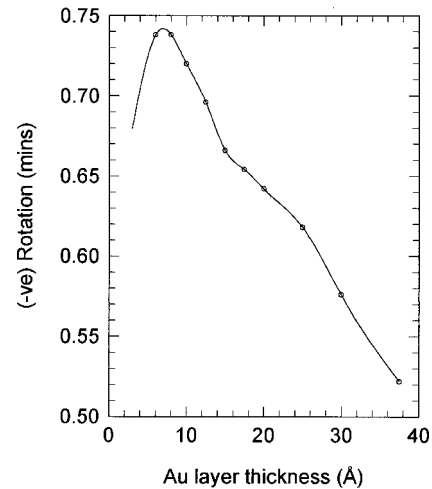
FIG. 13. Theoretical calculation of the complex Kerr rotation for a single bilayer (Co≡5 Å) with a Au buffer layer thickness of 300 Å.

appear as a magneto-optic oscillation, also of the same period. While the authors cannot demonstrate, directly, oscillations in the optical data, there is clear evidence of a variation in index that does lead to a prediction of a small oscillation in Kerr effect.

It remains, therefore, to explain the previously reported oscillations that have only been observed in Kerr rotation[9,20,21] and to reconcile this to both our own observations and to the proposed analysis. This will demonstrate the complete self-consistency of this approach and provide a challenging test for the model. To do this and for simplicity, we confine ourselves to the Au/Co/Au system reported here and also in Ref. 21. The most significant, and only, difference between the two experiments is the thickness of the buffer layer, in this case 125 Å, while previously it was reported to be 300 Å. As emphasized before, the optical environment of a magnetic layer may have a pronounced effect on the magneto-optic signals from the reflecting surfaces. To demonstrate this we have used our model and experimentally derived parameters to calculate the magneto-optical Kerr rotation expected for the system glass/300 Au/5 Co/0–37.5 Au. This corresponds to a single bilayer, but deposited onto the thicker Au buffer layer. The result is shown in Fig. 13 where, for the convenience of comparison with published curves,[21] the rotation has been inverted to match the previously unspecified sign convention. It is clear that the oscillations are now evident in the predicted rotation and that the general curve shape matches very closely with those previously reported. Those in ellipticity are much reduced and this will demonstrated experimentally. The ability of our analysis to explain this apparent anomaly is a significant achievement and further justification of the approach. To provide further evidence a final point is made by returning to our own magneto-optic data. Up to this stage the analysis has concentrated on the first three bilayers of the deposition. However, it should be remembered that a total of ten periods were deposited. It should be noted that since most of the material in the system is essentially Au, the thickness of the underlying material gradually increases as each successive period is added. Consequently, by the time the fifth period has been deposited, the effective buffer layer is comparable with that
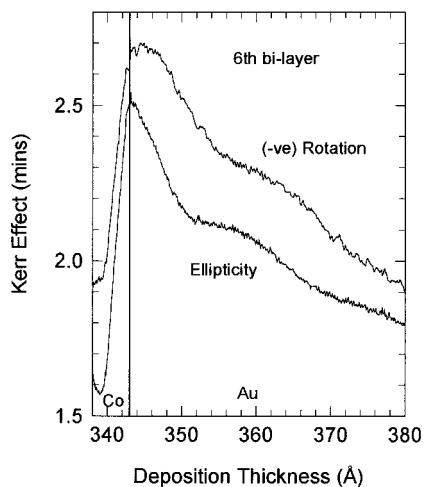
FIG. 14. Measurements of the complex Kerr effect for the sixth bilayer.

reported in Ref. 21. For this reason it is expected that the measured rotation will show evidence of oscillations and those for the ellipticity to be much reduced compared to those seen in Figs. 8 and 12. Figure 14 shows both the rotation and the ellipticity that were measured on deposition of the sixth bilayer. Again, the rotation has been inverted for comparison. It is abundantly clear that the observations are completely in accordance with expectations. Oscillations are seen in both rotation and ellipticity with the former being similar to previously reported curves and the latter very much reduced from those seen in the first bilayer. Any small differences may be accounted for by the fact that the underlying structure is, itself, magneto-optically active since it contains five individual Co layers. It is stressed that the characteristics of the curves of Fig. 14 are typical and are seen in the rest of the periods up to and including the tenth. This is expected since the underlying layer is now thicker than the optical skin depth.

The ability of the model to account for the oscillation in the complex Kerr effect (rotation and ellipticity) and its de-pendence on the underlying buffer layer thickness is significant and demonstrates the usefulness of the approach. One may, for example, design the underlying optical structure in order to maximise the amplitude of the oscillations in order to optimize the sensitivity of their observation.

V. CONCLUSIONS

A comprehensive optical and magneto-optical study of the growth dynamics of CoAu multilayers, using ellipsometry and Kerr polarimetry, has been carried out. It has been possible to determine values of effective optical and magneto-optical parameters for the Co and Au layers and to account for the general magneto-optical observations through calculations of the polar Kerr effect. Detailed examination of the Kerr ellipticity and rotations shows distinct oscillations with a spatial period of approximately 16 Å. Ellipsometric data, collected during the deposition of the Au layers, indicate a thickness-dependent refractive index that, when incorporated into the magneto-optical calculations, predicts the number and period of the oscillations seen in the ellipticity and their absence in the Kerr rotation when the buffer layer thickness is less than 125 Å. It is concluded that magneto-optical effects that are observed to oscillate with the thickness of a nearby noble-metal layer may be due to oscillations in the optical properties of the noble-metal layer and that, at least, the model suggested here, together with the optical and magneto-optical parameters, can be used to predict both the oscillatory nature of the complex Kerr effect and its magnitude irrespective of the optical environment or presence of additional underlying layers.

[1] W. B. Zeper, F. J. A. M. Greidanus, P. F. Carcia, and C. R. Fincher, J. Appl. Phys. **65**, 4971 (1989).

[2] R. Atkinson, S. Pahirathan, I. W. Salter, P. J. Grundy, C. J. Tatnall, J. C. Lodder, and Q. Meng, J. Magn. Magn. Mater. **162**, 131 (1996).

[3] S. S. P. Parkin, N. More, and K. P. Roche, Phys. Rev. Lett. **64**, 2304 (1990).

[4] M. N. Baibich, J. M. Broto, A. Fert, F. Van Dau Nguyen, F. Petroff, P. Etienne, G. Creuzet, A. Friederich, and J. Chazelas, Phys. Rev. Lett. **61**, 2472 (1988).

[5] B. Dieny, V. S. Speriosu, S. S. P. Parkin, B. A. Gurney, D. R. Wilhoit, and D. Mauri, Phys. Rev. B **43**, 1297 (1991).

[6] A. J. Freeman and R. Q. Wu, J. Magn. Magn. Mater. **104–107**, 1 (1992).

[7] R. Atkinson and P. M. Dodd, J. Magn. Magn. Mater. **173**, 202 (1997).

[8] S. Uba, I. Uba, A. Ya. Perlov, A. N. Yaresko, V. N. Antonov, and R. Gontarz, J. Phys.: Condens. Matter **9**, 447 (1997).

[9] T. Katayama, Y. Suzuki, M. Hayashi, and W. Geerts, J. Appl. Phys. **75**, 6360 (1994).

[10] W. R. Bennett, W. Schwarzacher, and W. F. Egelhoff, Jr., Phys. Rev. Lett. **65**, 3169 (1990).

[11] A. K. Zvedzdin and V. A. Kotov, *Modern Magneto-optics and Magneto-optic Materials* (IOP, London, 1997).

[12] R. Atkinson, P. J. Grundy, C. M. Hanratty, R. J. Pollard, and I. W. Salter, J. Appl. Phys. **75**, 6861 (1994).

[13] K. Sato, Jpn. J. Appl. Phys. **20**, 2403 (1981).

[14] R. Atkinson, J. Magn. Magn. Mater. **95**, 61 (1991).

[15] W. R. Hendren, Ph.D. thesis, Queen's University, Belfast, UK, 1995.

[16] S. Padovani, I. Chado, F. Scheurer, and J. P. Bucher, Phys. Rev. B **59**, 11 887 (1999).

[17] R. Atkinson and P. H. Lissberger, J. Magn. Magn. Mater. **118**, 271 (1993).

[18] R. Atkinson and P. H. Lissberger, Appl. Opt. **31**, 6076 (1992).

[19] J. E. Ortega, F. J. Himpsel, G. J. Mankey, and R. F. Willis, Phys. Rev. B **47**, 1540 (1993).

[20] Y. Suzuki, T. Katayama, P. Bruno, S. Yuasa, and E. Tamura, Phys. Rev. Lett. **80**, 5200 (1998).

[21] R. Mégy, A. Bounouh, Y. Susuki, P. Beauvillain, P. Bruno, C. Chappert, B. Lecuyer, and P. Veillet, Phys. Rev. B **51**, 5586 (1995).

[22] P. Bruno, Y. Susuki, and C. Chappert, Phys. Rev. B **53**, 9214 (1996).